JOURNAL OF GUIDANCE, CONTROL, AND DYNAMICS
Vol. 19, No. 2, March–April 1996

Nonlinear Inverse Dynamics Control of Aircraft Using Spoilers

X. D. Sun*
University of York, York Y01 5DD, England, United Kingdom
and
K. G. Woodgate† and J. C. Allwright‡
Imperial College, London SW7 2BY, England, United Kingdom

The nonlinear inverse dynamics (NID) methodology and its specific application to flight control using a promising control device, the spoiler, are studied. The proper control modeling of spoiler aerodynamics leads to a generic nonlinear model for the most typical aft-mounted spoilers that is then included in a complete nonlinear aircraft model. A novel systematic design procedure for the synthesis of robust NID-based flight control systems is presented. Use of the methodology for a modern combat aircraft, the Hawk trainer, leads to the development of a multimode longitudinal flight control system, with the particular aim of using spoilers as an active control device. Promising applications of spoilers for active control of aircraft are studied, and the related control configurations designed. Simulation results for aircraft maneuvering are presented, demonstrating the effectiveness of spoilers for aircraft maneuver enhancement and, in particular, in ameliorating the effects of wind shear and microbursts.

I. Introduction

THE complicated aerodynamic features and operational requirements of a modern aircraft present the control system designer with problems, typically nonlinearity, that are difficult to solve with conventional control system design approaches. The nonlinearity of an aircraft system exists in the dynamic equations and is closely connected with the flight condition. Its effects become severe when aircraft are undergoing an extreme maneuvering operation.[1] In addition, it may be introduced by the control system or by nonlinear control devices, such as spoilers.[2]

Spoilers are deflected plates, usually on the upper surface of a wing, that can be used to disturb the flow, causing separation and thereby changing the lift and drag of the aircraft. A popular and conventional arrangement of spoilers on the upper aft surface of a wing section can be seen in Fig. 1. As effective aerodynamic control surfaces, spoilers have been traditionally and widely used in aircraft control as speed brakes and/or as lift dumpers at touch down. They are also used as effective lateral control devices when asymmetrically deflected. A problem with spoilers as far as control is concerned is that the variable δ_{sp}, the deflection angle between spoiler and the wing, cannot be negative.

Recent experimental and computational studies in spoiler aerodynamics have suggested their potential usefulness for the active control of future aircraft, owing to their effectiveness in providing rapid force variation, the negligible changes in pitch moment, and their flexibility of use.[3–7] From the viewpoint of aerodynamics, the flowfield generated by a deflected spoiler on a wing can be very complicated and contains the phenomena of flow separation, reattachment, and vortex shedding.[2] Therefore, a spoiler exhibits more complex behavior than do most conventional aircraft control devices, such as the elevator, rudder, and aileron. Consequently, the modeling and complex control of aircraft become more difficult when spoilers are involved and demand innovative techniques.

There has been a great deal of progress in recent years in applying differential geometrical control theory to the linearization and control of a nonlinear system. The theory is relatively well developed and understood.[8] An important part of the theory and applications is the nonlinear inverse dynamics (NID) methodology, which uses input–output linearization via the construction of the inverse dynamics of a nonlinear system.[9] Its potential for flight control of aircraft has been demonstrated in many previous studies.

Early studies of the method were connected with system decoupling and separation of aircraft control modes.[10–12] Use of the method for an aircraft with complex characteristics and operational requirements, such as the power lift short takeoff and landing and vertical/short takeoff and landing was successfully carried out by Meyer.[13] During the same period, the method was applied to the control and testing of an aircraft flying through a large portion of the flight envelope.[14] In 1984, Meyer et al.[15] employed the method for the development of a helicopter control system, giving details of the construction of the transformation from the nonlinear system to the linear system. Recent work in this area includes that of Lane and Stengel,[16] who applied NID to the effective control of a 12-state nonlinear aircraft model in extreme flight conditions (high α and angular rates), and that of Hauser et al.[17] on the modified use of the method for the control of a nonminimum phase nonlinear aircraft system.

Because of the complex modeling of aircraft auxiliary control devices, such as flaps and spoilers, and their unexpected effect on the invertible dynamics,[13] their use for the active control of aircraft incorporating the NID has not been studied before. Although the feedback linearization methodology has received considerable attention in the literature and has found many applications in nonlinear flight control, little work on the robustness aspect of the nonlinear control systems has been documented.

These considerations are addressed in this paper, wherein the original contributions are 1) spoiler control modeling, generation of a generic spoiler model for flight control from experimental data; 2) design of flight control systems utilizing spoiler control, development of a NID-based robust control methodology that includes

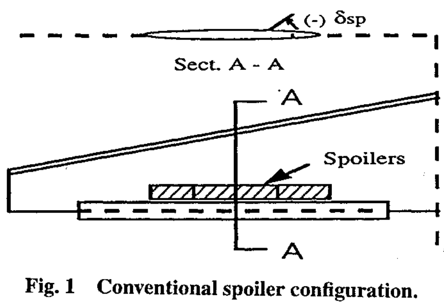

Fig. 1 Conventional spoiler configuration.

Presented as Paper 94-3592 at the AIAA Guidance, Navigation, and Control Conference, Scottsdale, AZ, Aug. 1–3, 1994; received Oct. 21, 1994; revision received Oct. 16, 1995; accepted for publication Oct. 28, 1995.

*Research Fellow, Department of Electronics.
†Lecturer, Department of Aeronautics.
‡Senior Lecturer, Department of Electrical and Electronic Engineering and Interdisciplinary Research Centre for Process Systems Engineering.

a parameter adaptive control algorithm to account for model uncertainties and its use for nonlinear control of the Hawk aircraft, with spoilers functioning as a principal control device; and 3) study and design of mission-defined longitudinal controllers for active use of spoilers for aircraft maneuver enhancement and gust/microburst alleviation.

II. Spoiler Control Modeling

A. General Remarks

The effects of spoilers are normally measured by integrated parameters, such as the lift, drag, and moment, that represent the effects on aircraft dynamics. Pressure and velocity distributions are also used to show the characteristics of the spoiler flowfield. The measurements of these parameters provide an understanding of spoiler flow mechanism and form the basis for the mathematical modeling of spoilers. As far as the use of spoilers for aircraft control is concerned, for precise modeling and introduction of spoilers into the control systems, comprehensive measurements of spoiler coefficients, $C_{l\mathrm{sp}}$, $C_{d\mathrm{sp}}$, and $C_{m\mathrm{sp}}$, and/or their derivatives $C_{l\delta s}$, $C_{d\delta s}$ and $C_{m\delta s}$, are of great importance.

Many studies in this area have been based on wing-spoiler/aerofoil-spoiler experiments and their outcomes, as summarized by Sun,[18] focusing on the measurements of the coefficients for two-dimensional aerofoils and conventional spoiler designs and location. Some general conclusions concerning the principal features of spoilers can be drawn:

1) Aft- and upper-wing mounted designs have been widely adopted for conventional use owing to their large range of effectiveness, particularly at negative wing incidence.

2) Generally speaking, for an aft-mounted spoiler, when incidence α varies within the normal region and the spoiler deflection angle δ_{sp} is beyond an insensitive region, nearly linear coefficient functions $C_{l\mathrm{sp}}(\delta_{\mathrm{sp}})$, $C_{d\mathrm{sp}}(\delta_{\mathrm{sp}})$, and $C_{m\mathrm{sp}}(\delta_{\mathrm{sp}})$ are obtained. The experimental data also strongly suggest that a linear description of spoiler effectiveness vs spoiler projection height [$\delta_{h\mathrm{sp}} = \sin(\delta_{\mathrm{sp}})$] may be even better for modeling purposes.

3) There is an increasing dependence of spoiler effectiveness on the incidence α as it approaches the stall regions (positive or negative).

4) An aft-mounted spoiler has an effect on the pitching moment of an aircraft, the extent of which depends heavily on the location of the spoiler. This effect may have a considerable influence on the longitudinal handling and control.

5) Under some circumstances and assumptions, two-dimensional aerofoil/spoiler data may be applied to the three-dimensional case.[4] Hence, we may initially design and tailor suitable spoilers for a wing by referring to relevant two-dimensional test data.

B. Design of a Generic Spoiler Control Model

With the aim of providing a precise mathematical expression of spoiler behavior when used as a control device, a generic spoiler control model for the most common location, aft mounted, is proposed. The design of the model is based on a recent series of experimental data concerning spoiler aerodynamics and is for a range of popular spoilers with the common feature of around 70% aerofoil profile chord ($\bar{c}$) location, a chord normalized to 10% aerofoil chord, and a span normalized to the whole span of the aerofoil. According to the spoiler data used for the modeling, the model would ideally be used for low-air-speed/Mach number cases with spoiler motion being quasisteady.[18]

The model expression takes the form of the related aerodynamic coefficients, namely, the spoiler lift coefficient $C_{l\mathrm{sp}}$, the drag coefficient $C_{d\mathrm{sp}}$, and the moment coefficient $C_{m\mathrm{sp}}$, and/or their derivatives relating to a linear model. In this study, a least-square error fitting (LSEF) technique in MATLAB™ (MathWorks, Inc.) was applied to the spoiler data, fitting algebraic expressions for the coefficients $C_{l\mathrm{sp}}$, $C_{d\mathrm{sp}}$, and $C_{m\mathrm{sp}}$. The spoiler deflection angle δ_{sp} and the wing incidence α appear as the most influential independent variables. The modeling process consisted of two major steps:

1) The spoilers were modeled for small aerofoil incidence, where the functional dependence of the spoiler effectiveness is mainly on its deflection angle δ_{sp}. The underlying mechanism is that, when the incidence is small or below some critical point, there is no interaction between separated wing flow and the spoiler-induced separation. Hence the effectiveness of the spoilers is decided solely by the separation because of their deflection. An important assumption was that spoiler effectiveness would be proportional to its projected height, which not only revealed the effect of spoiler chord length, leading to more collapsed data distributions suitable for the generic model, but also suggested an improved lift coefficient expression using the sine function.

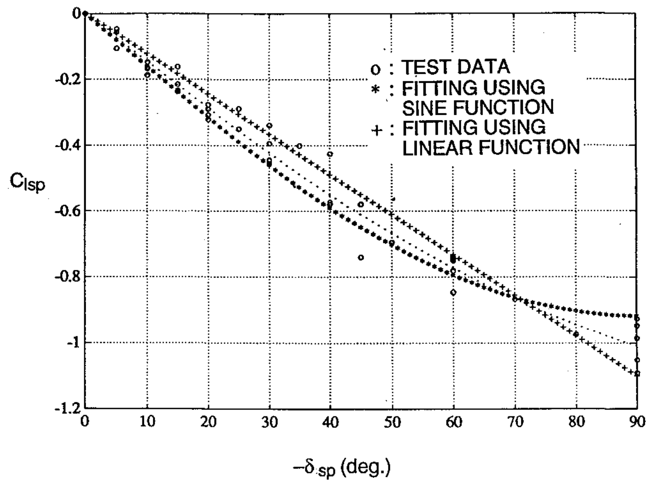

Fig. 2 $C_{l\mathrm{sp}}$ fitting from test data.

Figure 2 shows typical normalized spoiler $C_{l\mathrm{sp}}$ vs δ_{sp} data and different curve-fitting results for $C_{l\mathrm{sp}}$ using LSEF. The experimental data shown here are from those for spoilers with chords ranging from $5\%\bar{c}$ to $15\%\bar{c}$ (all normalized to $10\%\bar{c}$) and locations from $65\%\bar{c}$ to $73\%\bar{c}$. Linear fitting gives $C_{l\mathrm{sp}} = 0.7\delta_{\mathrm{sp}}$, with an error norm $EN = 0.45$, whereas fitting a sine function yields $C_{l\mathrm{sp}} = 0.92\sin(\delta_{\mathrm{sp}})$, with $EN = 0.41$.

2) The effect of incidence on spoiler effectiveness was introduced into the model, owing to the fact that the effectiveness of spoilers has an increasingly weak dependence on the deflection δ_{sp} as the wing incidence α approaches the positive or negative stall regions. This was made by defining an incidence influence function $\lambda(\alpha)$ and combining the function with the spoiler model from step 1:

$$\hat{C}_{\mathrm{sp}}(\alpha, \delta_{\mathrm{sp}}) = \lambda(\alpha) C_{\mathrm{sp}}(\delta_{\mathrm{sp}}) \tag{1}$$

where $\lambda(0) = 1$ yields $\hat{C}_{\mathrm{sp}} = C_{\mathrm{sp}}$, the spoiler model for small incidence cases. So, given $C_{\mathrm{sp}}|_{\alpha=0}$ and a family of $\hat{C}_{\mathrm{sp}}(\alpha, \delta_{\mathrm{sp}})$ curves, $\lambda(\alpha)$ can be modeled using piecewise linear interpolation of $\hat{C}_{\mathrm{sp}}/C_{\mathrm{sp}}$.

Applying this routine to the influence functions for the lift, drag, and moment coefficients, i.e., $\lambda_l(\alpha)$, $\lambda_d(\alpha)$, and $\lambda_m(\alpha)$ (with α in degrees), yields

$$\lambda_l(\alpha) = \begin{cases} 1 \\ \lambda_d(\alpha) = 1 - \alpha/15, \quad \lambda_m(\alpha) = 1 - \alpha/30, \quad -10 \le \alpha \le 20 \\ 2 - \alpha/10 \end{cases} \tag{2}$$

Finally, a nonlinear generic spoiler control model is given as

$$C_{l\mathrm{sp}} = 0.92\lambda_l(\alpha)\sin(\delta_{\mathrm{sp}}), \qquad C_{d\mathrm{sp}} = -0.1\lambda_d(\alpha)\delta_{\mathrm{sp}}$$

$$C_{m\mathrm{sp}} = -0.1\lambda_m(\alpha)\delta_{\mathrm{sp}} \tag{3}$$

where the functions $\lambda_l(\alpha)$, $\lambda_d(\alpha)$, and $\lambda_m(\alpha)$ are defined in Eqs. (2), (3), and (4), respectively, and $-90\ \mathrm{deg} \le \delta_{\mathrm{sp}} \le 0$ deg.

Based on the generic model, further analyses and evaluations of spoiler control effectiveness have been made[18] and, in particular, some artificial spoilers for the Hawk aircraft have been designed for advanced studies of active flight control utilizing spoilers.

III. Aircraft System Modeling

The general nonlinear aircraft model used here takes the form $\dot{x} = f(x, u)$, $y = C(x)$, with state variables $x \in \Re^n$, control inputs $u \in \Re^m$, and output variables $y \in \Re^q$. By augmenting the system dynamics with the derivatives of appropriate control inputs,[16] it can be transformed to

$$\dot{x} = A(x)x + B(x)u, \qquad y = C(x) \tag{4}$$

In most previous studies concerning nonlinear flight control using the feedback linearization methodology, control devices such as spoilers and flaps have not been considered. This was mainly because these devices were considered as only occasional and/or weakly coupled devices, and the incorporation of these direct force generators might result in a system that was not explicitly block triangular and, hence, not invertible.[13] Clearly, these arguments are not really valid and may result in an improper flight control when spoilers are actually active and in principal use.

In fact, in NID synthesis for longitudinal flight control where spoilers are principal control devices, where the measured variables are defined as $y_c = [V, \gamma, \alpha(\text{or}\,\theta)]'$, and where the controls are the elevator deflection δ_e, the thrust δ_t, and the spoiler deflection δ_{sp}, the introduction of the generic spoiler model as described in Sec. II into the aircraft model in Eq. (8) can be made through augmenting the aircraft system dynamics with the first derivative of the spoiler control input ($\dot{\delta}_{sp} = -a_{sp}\delta_{sp} + a_{sp}u_{sp}$; see Fig. 3), where the corresponding first-order lag represents, in practice, the spoiler actuator dynamics that can be expected to have a high bandwidth (e.g., $a_{sp} = 40$). To match the relative order of the longitudinal aircraft system with respect to the spoiler input, the system dynamics are augmented by a first-order lag in the thrust control, modeling the delay in the engine dynamics (e.g., $a_t = 0.5$).

Using a hybrid coordinate system consisting of mixed wind and body axes,[19] the foregoing procedure produces a complete aircraft longitudinal open-loop system, having the following two-dimensional 3-axis block lower-triangular form, with which the stable inverse dynamics can be constructed for the NID control laws[13]:

$$\begin{bmatrix} \dot{x}_1 \\ \dot{x}_2 \end{bmatrix} = \begin{bmatrix} A_1(x_1, x_2) \\ A_2(x_1, x_2) \end{bmatrix} + \begin{bmatrix} 0 \\ B_2(x) \end{bmatrix} u \tag{5}$$

where

$$x = \begin{bmatrix} x_1 \\ x_2 \end{bmatrix}, \qquad x_1 = \begin{bmatrix} V \\ \gamma \\ \alpha(\text{or}\,\theta) \end{bmatrix}, \qquad x_2 = \begin{bmatrix} q \\ \delta_t \\ \delta_{sp} \end{bmatrix}$$

$$u = \begin{bmatrix} u_e \\ u_t \\ u_{sp} \end{bmatrix}$$

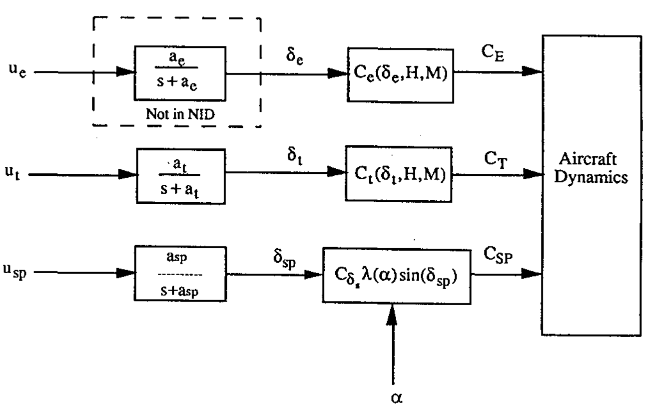

Fig. 3 System augmentation and actuator dynamics modeling.

$$A(x) = \begin{bmatrix} A_1(x_1, x_2) \\ A_2(x_1, x_2) \end{bmatrix} = \begin{bmatrix} -\dfrac{D}{m} - g\sin\gamma \\ \dfrac{(L - mg\cos\gamma)}{mV} \\ q - \dot{\gamma} \\ \dfrac{M}{I_{yy}} \\ -a_t\delta_t \\ -a_{sp}\delta_{sp} \end{bmatrix} \tag{6}$$

$$B_2(x) = \begin{bmatrix} b_{\delta_e} & 0 & 0 \\ 0 & a_t & 0 \\ 0 & 0 & a_{sp} \end{bmatrix}$$

and D, L, and M are the drag, lift, and pitch moments that are nonlinear functions of the aerodynamic coefficients and of the system variables,[20] V the flight-path velocity, γ the flight-path angle, α the incidence angle, q the rate of pitch angle θ, and u_e, u_t, and u_{sp} the control inputs for δ_e, δ_t, and δ_{sp}, respectively. Elevator effects were neglected when computing $A(x)$.

IV. Robust NID Controller Synthesis

A. New Procedure for NID Control Synthesis

The NID control synthesis was applied to the system model (9) to generate nonlinear controllers. During the process, a novel design procedure for simple yet effective formation of various mission-defined controllers was developed. One limitation of the procedure is that it applies only to systems for which $y = Cx$. However, this is commonly the case in flight control systems where the output to be controlled is usually some linear combination of state variables. The major steps of the procedure are as follows.

1) Find the m by n constant output matrix C such that $y = Cx$ where y is the vector of control output variables of interest chosen from $y_c = [V, \gamma, \alpha, q, \theta, \delta_t, \delta_{sp}]'$.

2) Calculate the Lie derivatives[9]

$$L_A x, \ldots, \left(\frac{\partial}{\partial x}\right)\left(L_A^{r_i - 1} x\right) A(x), \qquad \left(\frac{\partial}{\partial x}\right)\left(L_A^{r_i - 1} x\right) B(x)$$

for the inverse dynamics, where the derivative order r_i depends on the system model and the control variables. For the model of Eq. (9) and the selections of the group just given, $r_i = 2$ was used for x_1 and $r_i = 1$ for x_2. These can be viewed as the inverse dynamics matrices for the controller when unity C is selected, the so-called principal controller

$$u_p = B_p^*(x)^{-1}\left[v - A_p^*(x)\right]$$

where

$$A_p^*(x) = C\left[\frac{\partial}{\partial x}\left(L_{A_p}^{r_i - 1} x_p\right)\right] A_p(x)$$

$$B_p^*(x) = C\left[\frac{\partial}{\partial x}\left(L_{A_p}^{r_i - 1} x_p\right)\right] B_p(x)$$

$$x_p = x_1(\text{or}\,x_2)$$

3) Design multimission-defined controllers by simply assigning the output matrices C according to the mission objectives associated with the m control output variables and performing the following simple computations for the inverse dynamics matrices:

$$A^*(x) = CA_p^*(x), \qquad B^*(x) = CB_p^*(x) \tag{7}$$

When $B^*(x)$ is nonsingular, the control law is given by

$$u = B^*(x)^{-1}[v - A^*(x)] \tag{8}$$

We refer to Ref. 18 for a detailed presentation of A^* and B^*. The coefficients of the designed closed-loop pole polynomial for each

Table 1 Pole polynomial coefficients

Output variable Y	α_{i1}	α_{i2}
V	5.0	4.0
γ	3.0	4.0
θ	3.0	4.0
α	3.0	4.0

decoupled output variable were chosen with reference to the level-1 flight quality criteria of the Mil-F-8785C.[21] Table 1 lists typical data for the output control variables V, γ, θ, and α. These coefficients define the desired closed-loop systems whose flight qualities meet first-level specifications.

B. Design and Incorporation of NID-Based Parameter Adaptive Control Laws

Based on the NID controller design, an approach using a parameter adaptive control law (PACL) for the robustness of the designed nonlinear inverse dynamics flight control system (NIDFCS) was studied. The use of adaptive control is motivated by two considerations. First, the effectiveness of the desired NID control is heavily dependent on the modeling accuracy of the dynamical system to be controlled. An exact cancellation of all nonlinear terms must be obtained for the valid implementation of exactly linear control laws. If there is any uncertainty or error in the modeling process, and hence in the inverse dynamics formulation, the cancellation will not be exact and so the resulting control might not meet the design specifications. Second, it has become increasingly difficult to model precisely many modern technological systems, particularly high-performance aircraft with increased dynamic ranges, flight envelopes, nonlinearities, and complex aerodynamics. In aircraft flight control the robustness issue can become critical in certain worst cases.

The PACL used here aims to enhance the NID control robustness to parameter uncertainties in Eq. (9), where the system dynamics matrix $A(x)$ and the control matrix $B(x)$ can be put into the parametrized forms

$$A(x) = \sum_{i=1}^{n_1} \theta_{A_i} A_i(x) \tag{9}$$

$$B(x) = \sum_{j=1}^{n_2} \theta_{B_i} B_i(x) \tag{10}$$

where $\theta_{A_i}, i = 1, \ldots, n_1$ and $\theta_{B_i}, j = 1, \ldots, n_2$ are unknown parameters and the $A_i(x)$ and $B_i(x)$ are known smooth functions of state. Using the newly developed nonlinear parameter adaptive control theory,[22] a PACL for θ, which is of interest in aircraft dynamics, was developed and combined with the existing NID controllers to enhance the robustness of the NIDFCS to parameter uncertainties in the aircraft modeling.

The parameter adaptive control follows the procedure given next.

1) Define a polynomial $L(s) = s^r + a_1 s^{r-1} + \cdots + a_r$ such that $M(s) = L^{-1}(s)$ is strictly proper and stable. In many cases, $a_i, i = 1, \ldots, r$ may correspond to the desired closed-loop pole positions (see Table 1).

2) Calculate the error equation

$$\Phi' W = e^r + \alpha_1 e^{r-1} + \cdots + \alpha_r e \tag{11}$$

according to specified parameter adaptations. Here, the prime denotes matrix transposition, $\Phi = \hat{\Theta} - \Theta$, where $\hat{\Theta}$ is an estimate of the component vector of parameters Θ in Eqs. (13) and (14) and $e = y_m - y$, where y_m is the output from the modeled plant.

3) From the error equation, get the mismatch regressor W and then the intermediate variable $\zeta = M(s)W$.

4) From the measurement e, use of a normalized gradient-type algorithm[23] gives the update law

$$\dot{\Phi} = \frac{e_1 \zeta}{1 + \zeta' \zeta} \tag{12}$$

where $e_1 = e + \hat{\Theta} M(s) W - M(s) \hat{\Theta}' W$.

5) In the case of Θ being constant or its variation in the updating process being negligible, as is the case in most aircraft systems, we have

$$\dot{\hat{\theta}} = \dot{\Phi} \tag{13}$$

so that an update computation of $\hat{\theta}$ can be made via

$$\hat{\theta}_{k+1} = \hat{\theta}_k + \dot{\Phi} T \tag{14}$$

where T is the time step.

6) Go to step 3.

Initially, a single input/single output problem was formulated for the aircraft system with the elevator input δ_e as input and the pitch angle θ as output. In this case, the aircraft dynamics are

$$\dot{x} = \theta_{A_1} A_1(x) + \theta_{A_2} A_2(x) + \theta_B B(x) u, \qquad y = Cx \tag{15}$$

while the NID control refers to the following estimated model:

$$\dot{x} = \theta_{A_1} A_1(x) + \hat{\theta}_{A_2} A_2(x) + \hat{\theta}_B B(x) u, \qquad y = Cx \tag{16}$$

where $\hat{\theta}_{A_2}$ and $\hat{\theta}_B$ are the uncertain parameters. From the definition of input and output,

$$\dot{y} = \hat{L}_A C = C\left[\theta_{A_1} A_1(x)\right] \tag{17}$$

and the control based on the inaccurate model is

$$\hat{u} = \frac{-\hat{L}_A^2 C + \hat{v}}{\hat{L}_B \hat{L}_A C} \tag{18}$$

where

$$\hat{L}_A^2 C = C\left(\theta_{A_i}\right)^2 \frac{\partial A_1(x)}{\partial x} A_1(x) + C\theta_{A_1} \hat{\theta}_{A_2} \frac{\partial A_1(x)}{\partial x} A_2(x) \tag{19}$$

$$\dot{y} = \hat{u} = \frac{-\hat{L}_A^2 C + \hat{v}}{\hat{L}_B \hat{L}_A C} \tag{20}$$

$$\ddot{y} = C\left(\theta_{A_i}\right)^2 \frac{\partial A_1(x)}{\partial x} A_1(x) + C\theta_{A_1} \theta_{A_2} \frac{\partial A_1(x)}{\partial x} A_2(x) + C\theta_{A_1} \theta_B \frac{\partial A_1(x)}{\partial x} B(x) u \tag{21}$$

$$\hat{L}_B \hat{L}_A C = C\theta_{A_i} \hat{\theta}_B \frac{\partial A_1(x)}{\partial x} B(x) \tag{22}$$

Thus, the error equation for this case is

$$\ddot{e} + \alpha_1 \dot{e} + \alpha_2 e = \hat{v} - \ddot{y} = \begin{bmatrix} \Phi_{A_2} & \Phi_B \end{bmatrix} \begin{bmatrix} W_A \\ W_B \end{bmatrix} \tag{23}$$

where $\Phi_{A_2} = \hat{\theta}_{A_2} - \theta_{A_2}, \Phi_B = \hat{\theta}_B - \theta_B$, and

$$W_A = C\theta_{A_i} \frac{\partial A_1(x)}{\partial x} A_2(x) \tag{24}$$

$$W_B = C\theta_{A_i} \frac{\partial A_1(x)}{\partial x} B(x) \frac{-\hat{L}_A^{(2)} C + \hat{v}}{\hat{L}_B \hat{L}_A C} = C\theta_{A_i} \frac{\partial A_1(x)}{\partial x} B(x) \hat{u} \tag{25}$$

The PACL was applied where the uncertainty is in the most influential parameters in the longitudinal moment equation, typically the moment coefficient $C_{m\alpha}$ and the elevator control coefficient $C_{m\delta_e}$:

$$\Phi = [\Phi_{A_2} \quad \Phi_B], \qquad \Phi_{A_2} = \hat{C}_{m\alpha} - C_{m\alpha}, \qquad \Phi_B = \hat{C}_{m\delta_e} - C_{m\delta_e} \tag{26}$$

$$W = \begin{bmatrix} W_A \\ W_B \end{bmatrix}, \qquad W_A = a_{42}(x), \qquad W_B = b(x) \frac{\hat{v} - \hat{L}_A^{(2)} C}{\hat{L}_A \hat{L}_B C} = b(x) \hat{u}_e \tag{27}$$

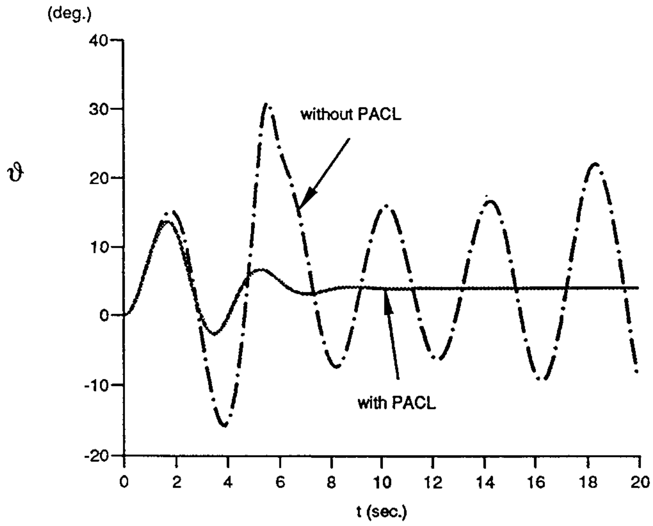

Fig. 4 Comparison of ϑ tracking: mode A1.

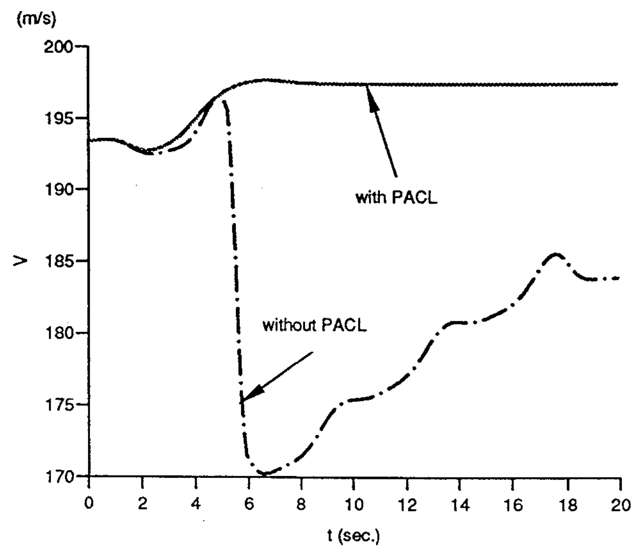

Fig. 5 Comparison of V tracking: mode A1.

where $b(x) = (\rho V^2 S\bar{c}\delta_e)/2I_{yy}$. Having calculated Φ and W, the parameter update procedure in Sec. IV was programmed and performed. For $y = \vartheta$, the quantity $L(s)$ was taken to be the same as the pole polynomial for the decoupled ϑ control.

The effectiveness of the PACL in enhancing NID robustness has been demonstrated in a series of simulations. Figures 4 and 5 present a comparison of system performance with and without PACL. Here, the actual aircraft was supposed neutrally stable with the stability coefficients $C_{m\alpha} = 0.0$ and $C_{m\delta_e} = -0.475$, whereas the initial estimated aircraft model for the NID control employed the nominal data $\hat{C}_{m\alpha} = -0.185$ and the reduced estimate $\hat{C}_{m\delta_e} = -0.2$.

The simulation shows that the NID control without PACL failed to control both ϑ (Fig. 4) and V (Fig. 5). Tracking the desired trajectories caused severe deterioration in stability (a violent oscillation) and aircraft handling. In sharp contrast, by applying PACL to the system, the stability of the aircraft was immediately restored after a short period of excitation for the parameter update and ϑ and V tracked the desired trajectories. Figure 6 shows the case where control mode B was applied with spoiler control. By comparing the cases with and without the use of PACL, it can be seen that even in the presence of the extra control input (the spoiler) that may excite the original oscillation in the multi-input/multi-output system, the designed adaptive control law still works properly and achieves an improved, robust, NID control for the aircraft.

C. System Configuration and Control Modes

The complete configuration of the NIDFCS is shown in Fig. 7. The design for the various mission-defined controllers of the Hawk

Table 2 Longitudinal control mode summary

Control mode	Output control variables	Mission objectives
A (conventional)		
A1 (controller 4*)	$[V\theta]$	Cruising
A2 (controller 5)	$[V\alpha]$	Conventional trajectory maneuvering
B (unconventional)		
B1 (controller 6)	$[\theta\gamma]$	Unconventional level flight decelerating
B2 (controller 1)	$[V\gamma\theta]$	Decoupled V, γ, θ maneuvering (takeoff and landing)
B3 (controller 2)	$[V\gamma\alpha]$	Decoupled V, γ, α maneuvering
B4 (controller 3)	$[V\alpha\theta]$	Decoupled V, θ, α maneuvering

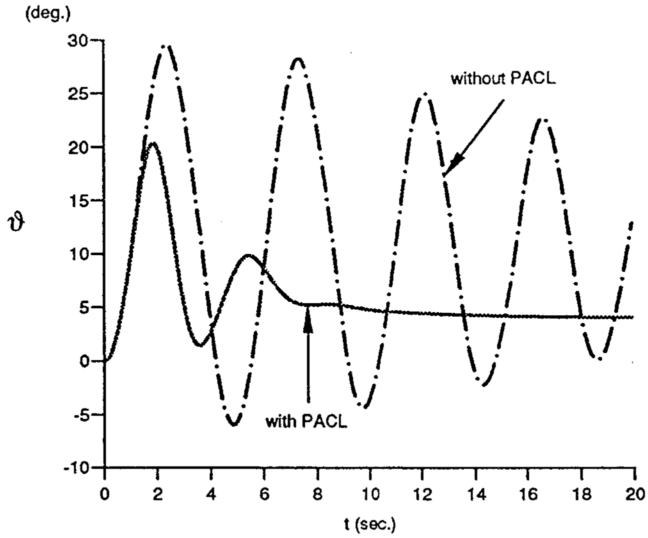

Fig. 6 Comparison of ϑ tracking: mode B1.

aircraft resulted in a multimode flight control system. Table 2 summarizes some of the major control modes, where class A is for conventional control and class B is for unconventional control. The modes A1 and A2 are for the conventional control augmentation in aircraft velocity and attitude whereas B1–B4 are the control modes utilizing the spoiler control for various unconventional control purposes. The mission objectives for which a control mode is expected to be applicable are listed in the right-hand column of the table.

V. Aircraft Performance Enhancement Using Spoilers

The preceding development of the NIDFCS provides the basis for active control of aircraft using spoilers. With regard to the spoiler control potential and its significant role in flight control, three special application cases are of particular interest: 1) decoupled attitude and trajectory control for superior maneuver of aircraft that utilizes the unique control effect of spoilers on the flight path, 2) fast deceleration control that takes advantage of significant spoiler drag, and 3) control augmentation for gust/turbulence and microburst alleviation that benefits from the spoiler feature of rapid force variation. The following gives a detailed example of the use of spoilers for the third objective.

Wind shear is a local, transient change in the wind vector that brings a rapid and highly influential change in the airflow over the aerodynamic surface of an aircraft. A form of wind shear that is of particular concern to flight safety is the microburst, in which a large mass of air is propelled downward in a jet form from some convective fields and/or a rapid buildup of small weather cells. An intense microburst can produce about 70-m/s (150-mph) horizontal winds as well as 20-m/s (48-mph) down flows at treetop levels.[24] Such a violent and invisible change in wind velocity presents the greatest danger to aircraft flying at low altitudes and at low speeds. It is believed to be the real cause of many aircraft accidents during

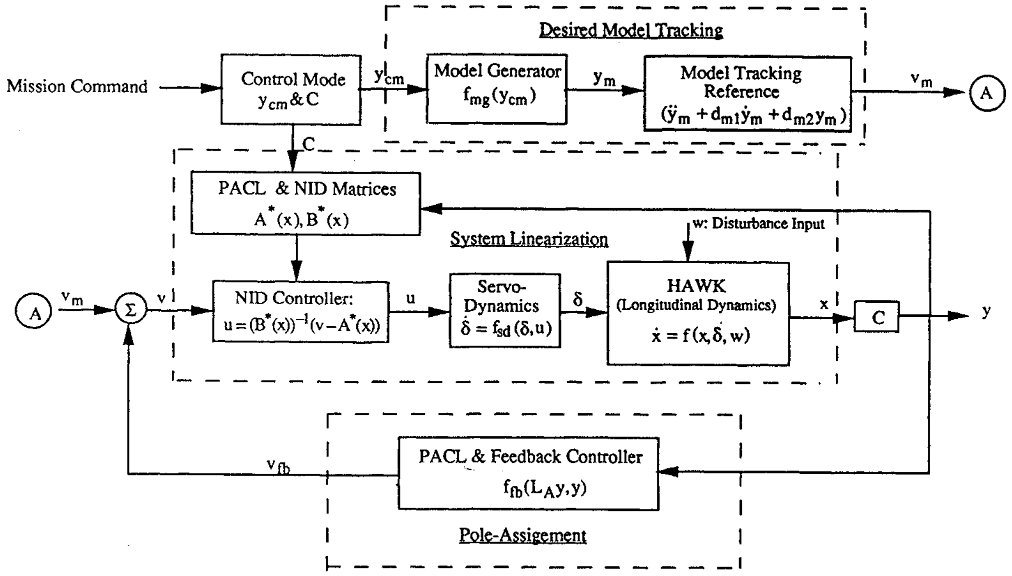

Fig. 7 NIDFCS configuration.

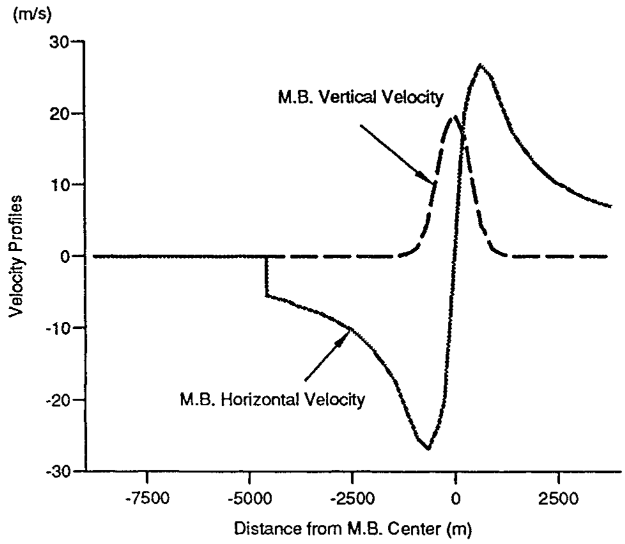

Fig. 8 Microburst model and distribution.

landing and takeoff phases, e.g., the crash of a Beoing 727 at JFK airport in New York in June 1975.[25]

A special spoiler control for microburst alleviation for an aircraft penetrating a severe microburst during approach to landing was designed and evaluated by simulation. The control programming is characterized by direct countering of the microburst impacts using the fast and direct force control from spoilers and differs from most previous studies concerning microbursts where emphasis was put on avoidance and escape procedures.[26]

A. Microburst Model

A two-dimensional microburst model by Melo and Hansman[26] was used in this study, with the maximum intensity horizontal and vertical velocity profiles presenting a worst case. The model was based on the Andrews Air Force Base event in 1983 with the maximum horizontal velocity of 27 m/s and the maximum vertical velocity of 20 m/s (Fig. 8).

B. Spoiler Control Logic

Based on the spoiler control model already defined, the control model B1 for fast deceleration control was chosen for the deceleration control prior to the landing approach and for a presetting of the balance angle of the spoiler that enables the spoiler to act as a bidirectional control device while encountering the microburst. Then the control mode B2 was applied for the trajectory control augmentation.

Table 3 Maximum deviatioin comparison

	Case A	Case B	Case C
$\lvert dH \rvert_{max}$, m	Impact (t = 94 s)	150	30
$\lvert dX \rvert_{max}$, m	Impact	2470	610
$\lvert dV_{max} \rvert$, m/s	Divergence	1.3	2.6
$\lvert d\gamma_{max} \rvert$, deg	24	9.5	3.5

C. Simulation

The simulations of the penetrating flight through the microburst were programmed in three stages as follows: 1) starting from a low-altitude balanced flight at H_0 = 1000 m, V_0 = 193 m/s; 2) decelerating the flight from V_0 to the desired descent speed V_d = 120 m/s; and 3) performing the landing approach following the desired gliding trajectory with the output variables as V_d = 120 m/s (268 kn) and $\gamma_d = -3$ deg, which correspond to a descent rate of $\dot{H}_d$ = 6.3 m/s. The desired trajectory is shown in Fig. 9. The microburst was introduced to the approach process through the variables $V_{wg}(X)$ and $V_{ug}(X)$, with the microburst center located at X = 8900 m from the start point of the simulations. The simulation duration was 100 s, with the deceleration time automatically set by the reach of the desired approaching speed (V_d = 120 m/s, t = 22 s). The desired terminal height was H_{dt} = 500 m.

Three cases of control and augmentation were applied to the microburst penetrating flight and their effects were compared to one another. The three cases were case A, programmed flight without control augmentation, with the control inputs preset; case B, integrated pitch and velocity control augmentation, using control mode A1; and case C, integrated pitch and trajectory control augmentation, using control mode B2.

D. Evaluation

Table 3 summarizes the maximum deviations from the desired trajectory, in the principal state variables of H, X, V, and γ in the three microburst-penetration flights, whereas Figs. 9, 10, and 11 present comparisons of the trajectory $H(X)$, the path velocity $V(t)$, and angle $\gamma(t)$ among the three cases, respectively.

From the simulations and evaluation, it can be seen that severe microbursts are, indeed, a great threat to aircraft flying at low altitudes and low speeds, e.g., takeoff and landing phases. Even for an aircraft such as the Hawk that possesses a very desirable natural stability at low altitudes,[18] without augmentation and precaution measures the worst microburst simulated may result in a greater than 500-m loss in height from the desired flight trajectory halfway to touchdown and large divergences in the major variables; there is no doubt that microbursts present one of the gravest dangers to both commercial and military aircraft.

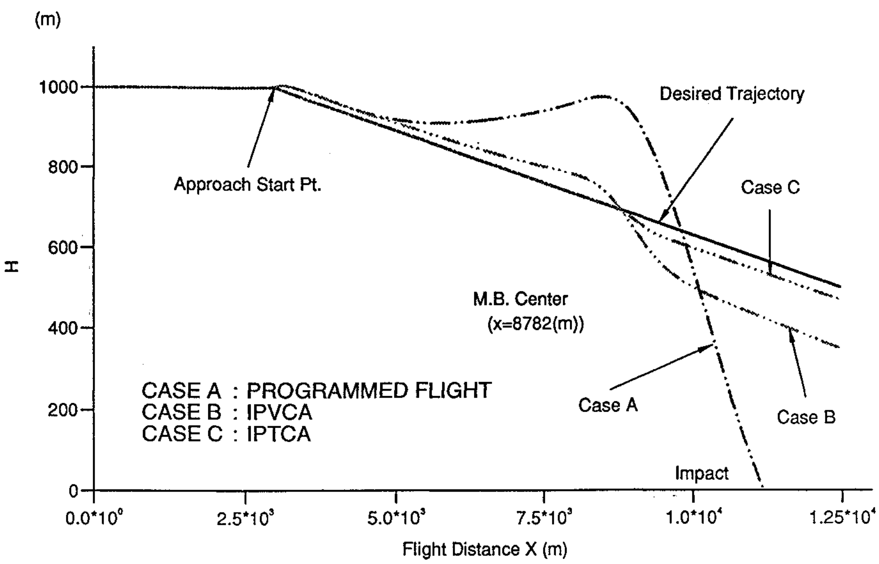

Fig. 9 Comparison of flight trajectories in microburst penetration.

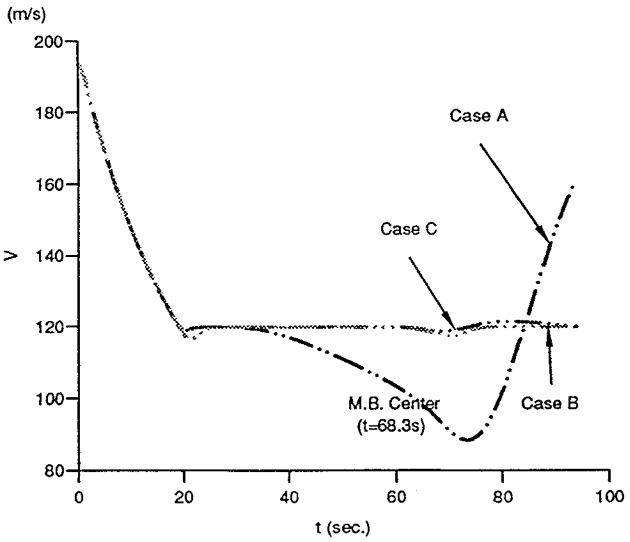

Fig. 10 Comparison of flight-path velocity responses.

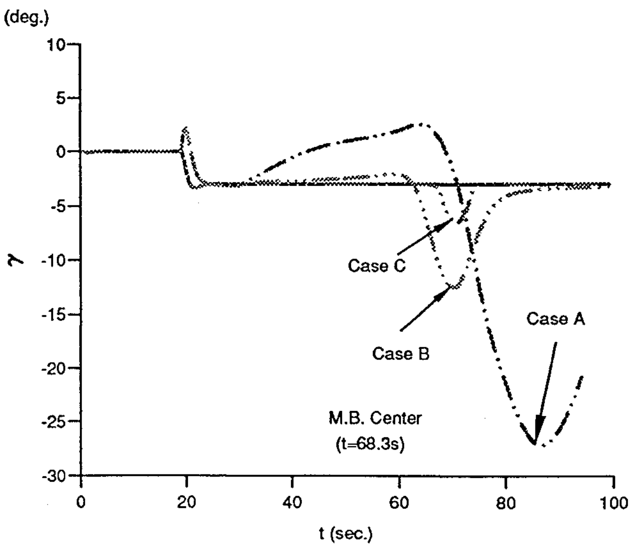

Fig. 11 Comparison of flight-path angle responses.

Although conventional augmentation control using the elevator and thrust brought about a considerable improvement in stability during penetrating flight, the most beneficial control augmentation resulted from the introduction of the spoiler, because of its unique effect on the fast and direct suppression of the force impacts of the microburst and on precise trajectory keeping. By appropriately choosing the control mode and offsetting the spoiler deflection angle (-70 deg in this case), use of the spoiler control gave a good and almost deviation-free augmentation in H, V, and γ and substantially improved results over the conventional control, thereby improving the safety and performance levels of the aircraft.

VI. Concluding Remarks

Previous work on spoiler aerodynamics has demonstrated the potential of spoilers in future aircraft. This study is the first attempt at a systematic control study of spoilers using the NID methodology. It concerns the modeling, control configuration, and active use of spoilers for flight control. The work has shown that the generic model proposed does indeed provide a logical, practical, and yet also flexible way for representing the major control features of spoilers. The model can be used easily in different flight control studies and system developments.

System development using inverse dynamics has again been demonstrated to be an effective method for synthesizing nonlinear controllers and generating a decoupled, multimode control system for the Hawk aircraft. In this study, a new design procedure for the use of NID control was developed, with novel features including the principal controller-based multicontroller design, the direct incorporation of flight quality specifications within the controller syntheses, and the incorporation of system robustness enhancement via parameter adaptive control. A successful application example of the methodology has been to the Hawk NID flight control system.

The application of spoilers for active aircraft control has demonstrated that the introduction of spoilers enhances the stability and control of aircraft and may well be applicable to mission objectives requiring superior maneuvering and/or precise trajectory control and stabilization. In particular, we studied the case of using spoilers for alleviation of the effects of microbursts and designed nonlinear controllers for this purpose. The simulations show promising results in ameliorating the hazards of microburst penetration during the landing phase.

All of these aspects of the study provide insight into spoiler control effectiveness and show that the introduction of spoilers does enhance the stability and control of aircraft and that their role in the active control of future aircraft appears promising.

Acknowledgments

The research of the first author was supported by the Technical Cooperation Training award of the British Council and by the Educational Committee of the People's Republic of China. We thank J. M. R. Graham and D. J. Doorly of the Department of Aeronautics, Imperial College, for many helpful discussions.

References

[1]Huang, C. Y., and Knowles, G. J., "Application of Nonlinear Control Strategies to Aircraft at High Angle of Attack," *Proceedings of the 29th IEEE Conference on Decision and Control* (Honolulu, HI), Inst. of Electrical and Electronics Engineers, New York, 1990, pp. 188–193.

[2]Mack, M. D., Seetharam, H. C., Kuhn, W. G., and Bright, J. T., "Aerodynamics of Spoiler Control Devices," AIAA Paper 79-1843, July 1979.

[3]Consigny, H., Gravelle, A., and Molinaro, R., "Aerodynamic Characteristics of a Two-Dimensional Moving Spoiler in Subsonic and Transonic Flow," *Journal of Aircraft*, Vol. 21, No. 9, 1984, pp. 687–693.

[4]Wentz, W. H., Jr., Ostowari, C., and Seetharam, H. C., "Effects of Design Variables on Spoiler Control Effectiveness, Hinge Moments and Wake Turbulence," AIAA Paper 81-0072, Nov. 1981.

[5]Parkinson, G. V., and Yeung, W., "A Wake Source Model For Aerofoils with Separated Flow," *Journal of Fluid Mechanics*, Vol. 179, June 1987, pp. 41–57.

[6]Costes, M., Gravelle, A., Philippe, J. J., Voges, S., and Triebstein, H., "Investigation of Unsteady Subsonic Spoiler and Flap Aerodynamics," *Journal of Aircraft*, Vol. 24, No. 9, 1987, pp. 629–637.

[7]Dystuynder, R., "Multi-Control System in Unsteady Aerodynamics Using Spoilers," AIAA Paper 87-0855, Jan. 1987.

[8]Isidori, A., *Nonlinear Control Systems*, Springer–Verlag, Berlin, 1989, p. 479.

[9]Akhrif, O., and Blankenship, G. L., "Using Computer Algebra for Design of Nonlinear Control Systems," Thesis Rept. M.S. 87-2, Univ. of Maryland, College Park, MD, Sept. 1987.

[10]Singh, S. N., and Rugh, W. J., "Decoupling in a Class of Nonlinear Systems by State Variable Feedback," *Journal of Dynamic Systems, Measurement and Control*, Vol. 94, 1972, pp. 323–329.

[11]Asseo, S. J., "Decoupling of a Class of Nonlinear Systems and Its Application to an Aircraft Control Problem," *Journal of Aircraft*, Vol. 10, No. 12, 1973, pp. 739–747.

[12]Freund, E., "The Structure of Decoupled Nonlinear Systems," *International Journal of Control*, Vol. 21, No. 3, 1975, pp. 443–450.

[13]Meyer, G., and Cicolani, L., "Application of Nonlinear System Inverses to Automatic Flight Control Design—System Concepts and Flight Evaluations," AGARDograph 251, Theory and Applications of Optimal Control in Aerospace Systems, Paper 10, 1981.

[14]Wehrend, W. R., Jr., and Meyer, G., "Flight Tests of the Total Automatic Flight Control System (TAFCOS) Concept on a DHC-6 Twin Otter Aircraft," NASA TP-1513, Feb. 1980.

[15]Meyer, G., Su, R., and Hunt, L. R., "Application of Nonlinear Transformations to Automatic Flight Control," *Automatica*, Vol. 20, No. 1, 1984, pp. 103–107.

[16]Lane, S. H., and Stengel, R. F., "Flight Control Design Using Nonlinear Inverse Dynamics," *Automatica*, Vol. 24, No. 4, 1988, pp. 471–483.

[17]Hauser, J., Sastry, S., and Meyer, G., "On the Design of Nonlinear Controllers for Flight Control Systems," AIAA Paper 89-3489, April 1989.

[18]Sun, X. D., "Active Control of Aircraft Using Spoilers," Ph.D. Thesis, Dept. of Aeronautics, Imperial College, London, March 1993.

[19]Etkin, B., *Dynamics of Atmospheric Flight*, Wiley, New York, 1972, p. 579.

[20]Herd, J., "Digital Simulation Techniques for a Fixed-Wing Aircraft," Dept. of Aeronautics, Imperial College, 3rd Year Rept., London, June 1985.

[21]Moorhouse, D. J., and Woodcock, R. J., "Background Information and User Guide for MIL-F-8785c Military Specification—Flying Qualities of Piloted Airplanes," U.S. Air Force Wright Aeronautical Labs., AFWAL TR-81-3109, Wright–Patterson AFB, OH, 1982.

[22]Sun, X. D., and Woodgate, K. G., "Robustness Enhancement of Nonlinear Inverse Dynamics Based Flight Control Systems," *Proceedings of the IFAC Symposium on Robust Control Design* (Rio de Janeiro, Brazil), 1994, Pergamon, Oxford, England, UK, pp. 441–446.

[23]Sastry, S., and Shankar, S., "Adaptive Control of Linearizable Systems," *IEEE Transactions on Automatic Control*, Vol. AC-34, Nov. 1989, pp. 1123–1131.

[24]Bowles, R. L., and Forst, W., "Wind-Shear/Turbulence Inputs to Flight Simulation and Systems Certification," NASA CP-2474, May 1987.

[25]McLean, D., *Automatic Flight Control Systems*, Prentice–Hall, Englewood Cliffs, NJ, 1990.

[26]Melo, D. A., and Hansman, R. J., Jr., "Analysis of Aircraft Performance During Lateral Maneuvering for Microburst Avoidance," *Journal of Aircraft*, Vol. 18, No. 12, 1991, pp. 837–842.